Joanes Berasategi et al 2018 Smart Mater. Struct. 27 045011

Fe nanoparticles produced by electric explosion of wire for new generation of magneto-rheological fluids

Joanes Berasategi [a)], Ainara Gomez [a)], M. Mounir Bou-Ali [a)] Jon Gutiérrez [b,c)], Jose Manuel Barandiarán [b,c)], Igor V. Beketov [d,e)], Aleksander P. Safronov [d,e)] and Galina V. Kurlyandskaya [b,d)]

[a)] *Mechanical and Industrial Production Department, Faculty of Engineering, Mondragon Unibersitatea, Loramendi 4, E-20500 Arrasate-Mondragón, Spain*

[b)] *Dept. of Electricity and Electronics, Universidad del País Vasco/Euskal Herriko Unibertsitatea, Faculty of Science and Technology, P. Box 644, 48080 Bilbao, Spain*

[c)] *BCMaterials, Parque Científico de Leioa, Sarriena 48160 Leioa, Spain*

[d)] *Ural Federal University B.N. Yeltcyn, Institute of Natural Sciences and Mathematics, Mira 19, 620002 Ekaterinburg, Russian Federation*

[e)] *Institute of Electrophysics Ural Division RAS, Amundsen str. 106, 620016, Ekaterinburg, Russian Federation*

Abstract

Iron magnetic nanoparticles have been produced by the technique of the electric explosion of a wire (EEW). The major crystalline phase (95 ± 1%) was α-Fe with lattice parameter a = 0.2863(3) nm. The size of coherent diffraction domains of this phase was 77 ± 3 nm. The EEW MNPs presented a large saturation magnetization value, reaching about 87 % of the saturation magnetization of the bulk iron. EEW NMPs demonstrated an improved magnetic performance when used in Magnetorheological (MR) Fluids with respect the commercial carbonyl iron particles (CIP) micron sized particles studied for comparison. The MR fluids composed with the EEW nanoparticles show larger yield stress values than those with CIP micron sized particles, so proving that the EEW MNPs have a high potential for MR fluids applications.

Keywords: Iron magnetic nanoparticles, magnetorheological fluid, electric explosion of wire

Introduction

Magnetic nanoparticles (MNPs) were intensively studied in recent years in a view of their versatile properties requested by very different applications including electronic, microwave and magnetorheological devices [1-3]. One of the most important factors limiting MNPs utilization in technological and biomedical applications is the small size of the batch. Electric explosion of a wire (EEW) is an electrophysical technique based on the overheating up to evaporation of a metallic wire by an electric high power pulse in a controlled inert atmosphere [4-5]. It yields spherical MNPs at production rates up to 200 g/h providing up to a kilogram in a single batch [6-7].

Although some of the EEW MNPs were successfully tested in small quantity for fabricating iron oxide-based or iron ferrofluids (FF) and MNPs/polymer composites [3, 7, 8], one can expect a larger potential in the field of smart materials were a large amount of MNPs is requested, i.e. for fluids, elastomers and foams whose mechanical properties can be controlled by the external magnetic field [8]. Magnetorheological (MR) fluids consist of stable suspensions of magnetic particles in a carrying fluid. Their reversible rheological behaviour can be modified by application of an external magnetic field. As a result, the behaviour of MR fluids (also called “intelligent” fluids) can be adapted to variable working conditions [9]. MR devices have the potential to create a new generation of valves, active shock/vibration dampers, hydraulic systems, actuators, and other parts of mechanical systems. At present, there is a extended technological request in developing a new and improved MR fluids in large quantities, having lower production cost and smaller ecological impact onto environment [3,9].

The first classification of the magnetic fluids proposed the concept of the particle size. According to Charles [10] the magnetic fluids can be classified in two main groups: FF and MR fluids. Whereas ferrofluids are composed by nanometric magnetic particles, MR fluids are dispersions of micron-sized particles. Further development of fabrication techniques showed that all properties of magnetic fluids depend critically on the fabrication technique, particles parameters, including fine features of the particle size distribution. Furthermore, the development of the advanced electrophysical techniques (such as laser target evaporation, arc plasma and EEW techniques) lead to the attempts to obtain MR fluids with very small iron MNPs of the order of 20 nm [11] or quite large iron particles of the order of 1000 nm, i.e. in a boarder size range than in the above mentioned classification [12].

The rheological behaviour of MR fluids, when subjected to an external magnetic field, is determined by a yield stress. The attractive interaction between the magnetic dipoles induced in the particles gives rise to chain-like structures directed along the field. This very fast transition from a liquid to almost solid state takes place in a fraction of millisecond time. A finite stress is needed for chain-like structures to form. The magnitude of this yield stress can be continuously controlled by the magnetic field intensity, and can reach a large magnitude due to the high magnetic saturation [9, 12]. In contrast, the rheological behaviour of ferrofluids is nearly Newtonian, with yield stress values drastically reduced in comparison to MR fluids. Inferior yield stress values of FF are explained by the lower magnetic saturation typical for nanoparticles [7, 13], caused by their oxidation during the synthesis process and much higher surface-to volume ratio [14, 15].

The colloidal stability of magnetic fluids is the most critical parameter for the consistent performance of any MR device [16]. FF present good stability, due to the size of the MNPs, as the Brownian effect is sufficient to prevent the particle's sedimentation [10]. On the other hand, the MR fluids present the intrinsic problem of particle sedimentation [13]. The successful strategy for the reduction of the particles aggregation and sedimentation is to use an stabilizing agent. In this context, although several works have been carried out in recent years analysing different compositions for enhanced MR fluids stability, the stability problem has not been fully solved yet [17-20].

With this respect the technique of electric explosion of a wire, which allowed fabrication a large amount of iron MNPs, seems to be very promising [21]. There are different possibilities of passivation of the surface of the fabricated nanoparticles with a protection carbon layer or a thin layer of iron oxide that avoids further oxidation of the core of the MNPs [22]. Consequently, spherical nanoparticles with high magnetic saturation can be obtained in large quantities.

In this work, pure iron nanoparticles were obtained by electric explosion of wire in order to evaluate their potential use in MR fluids. For sake of comparison two types of MR fluids have been designed on the basis of two different kinds of magnetic particles. The EEW iron MNPs and the commercially available micron sized carbonyl iron particles (BASF, Germany). The thorough comparison of the rheological behaviour of the two fabricated fluids, and the analysis of the data available in the literature indicated that the EEW MNPs have a noteworthy potential for use in MR fluids.

2. Experimental

2.1. Fabrication and characterization of EEW MNPs

Iron nanoparticles were synthesized using EEW equipment designed at the Institute of Electrophysics of RAS (Ekaterinburg, RF) [5, 22-26]. The EEW installation included an explosion chamber, a gas trap for separation of large particles and a filter for the accumulation of fine particles of the produced nanopowder. The installation was filled with a mixture of nitrogen (30%) and argon (70%) at 0.12 MPa. Circulation of the working gas with a flow of 150 l/min was provided by a gas turbine. In this system the purity of the fabricated particles is limited exclusively by the purity of the metal wire. A steel wire of low carbon content (0.07 wt. %) with 0.47 mm diameter was continuously fed into the explosion chamber from a roll, and 30 kV voltage pulses were repeatedly applied to a 89 mm portion of the wire. Pulse duration was 2 μs. The electrical energy passed through the portion of wire during each pulse provided 130 % excess energy with respect to the energy of sublimation of the metallic iron (424 KJ/mol). It resulted in the vaporization of the wire and the subsequent condensation of spherical metallic iron MNPs in the gas phase. The produced nanopowder was collected in the filter and removed from it after passivation by oxygen with a flow rate of 0.5 cm^3/s. The detailed description of EEW method can be found elsewhere [5, 7, 22-26].

XRD analysis was performed using Bruker DISCOVER D8 diffractometer operating with Cu-Kα radiation (λ = 1.5418 Å). Quantitative analysis was done using TOPAS-3 software. The average size of coherent diffraction domains was estimated using the Scherrer approach [27]. Electron microscopy characterization of the Fe MNPs was performed by scanning electron microscopy (SEM) (JEOL JSM-6400 operated at 20 kV) and transmission electron microscopy (TEM) (JEOL JEM2100 operated at 200 kV).

Specific surface area of the MNPs was measured by low-temperature nitrogen adsorption (Brunauer-Emmett-Teller physical adsorption (BET)) using a Micromeritics TriStar3000 analyser.

2.2. Synthesis of the Magnetic Fluids

Due to the high surface activity of the nanoparticles they strongly tend to form aggregates in suspensions and this aggregation is one of the main problems in processing air-dry nanopowders for re-dispersion in a liquid suspension. In this work two magnetic fluids have been designed with two kinds of magnetic particles of iron: EEW MNPs and the commercially available micron sized carbonyl iron particles (CIP) (HS grade, BASF, Germany) [28]. The thorough comparison of the rheological behaviour of the two fabricated fluids, and analysis of the available in the literature data indicated that the EEW MNPs have a noteworthy potential for use in MR fluids. Mineral oil (pure grade, ACROS, Belgium) was used as carrier fluid. Two suspensions were prepared using a 10% solid volume fraction from the EEW and CIP particles. To prepare the suspensions, proper amounts of carrier liquid, thickening agent Lubrizol ®3702 (0.95 wt%, Lubrizol, EEUU) and aluminium stearate surfactant (0.3 wt%, technical grade, Fluka, EEUU) were mixed first by hand stirring and then by ultrasonic treatment. Half of the proper amount of particles was added to the suspension during mechanical stirring. After that, the suspension was homogenized in the ultrasonic bath for 2 minutes. This process was repeated by the addition of the remaining particles. The final suspension was treated for 24 hours in the mechanical stirrer to reach the desired homogeneity.

2.3. Magnetic and magnetorheological characterization

Magnetic measurements of the air-dry particles were performed at room temperature by a vibrating sample magnetometer (VSM) in magnetic fields up to 2 Tesla, which is high enough for reaching the magnetic saturation of the samples. Few mg of the powders were carefully weighted and fixed in the gelatine capsule.

Magnetorheological characterization has been carried out by an Anton Paar Physica MCR 501 rotational rheometer equipped with the MRD70/1T magnetorheological cell and the parallel disk configuration (PP20/MRD/TI/P2).

3. Results and discussion

3.1. Structural characterization

XRD analysis of EEW MNPs confirmed that the major crystalline phase (95 ± 1%) was α-Fe, cubic fcc (face cubic centered, S.G: Im-3m, see Figure 1) with lattice parameter a = 0.2863(3) nm. The size of the coherent diffraction domains of this phase was 77 ± 3 nm. Two minor phases were found: 2 ± 1% of γ-Fe**,** cubic bcc (body cubic centered S.G: Fm-

3m) with lattice parameter a = 0.3592(2) nm and 3 ± 1% of magnetite (S.G: Fd-3m) with lattice parameter a = 0.8360(6) nm. The size of the coherent diffraction domains for γ-Fe was 32 ± 9 nm, and 9 ± 2 for magnetite. Thus, it is reasonable to conclude that γ-phase might be associated with small MNPs in the ensemble of iron nanoparticles and the magnetite phase corresponds to the passivation layer on the surface of MNPs.

Figure 1

SEM and TEM images given in Figure 2 show that Fe MNPs were spherical and non-agglomerated. Particle size distribution (PSD) was obtained by image analysis of SEM and TEM micrographs. PSD is given in the inset in Figure 2. PSD is fitted well by lognormal distribution function with median 85 nm and logarithmic dispersion 0.378. The median of PSD correlates well with the average size of coherent diffraction domains for α-Fe phase.

Figure 2

Specific surface area of Fe MNPs was measured by low-temperature nitrogen adsorption (Brunauer-Emmett-Teller physical adsorption (BET)) using Micromeritics TriStar3000 analyser. It was 7.2 m^2/g. The value of the specific surface area of the spherical particles (S_{sp}) is geometrically related to the average particle diameter (D_{BET}) according to equation [29]:

$$D_{BET} = \frac{6}{\rho S_{sp}} \quad (1),$$

where ρ is the density of Fe (7.8 g/cm^3). The calculated value of D_{BET} was 106 nm, in fair agreement with the median of PSD and the average size of coherent diffraction domains. The most likely reason for the small deviation is the underestimation of the fraction of large particles in the ensemble. It is noticeable from the inset in Figure 2 that lognormal PSD gives lower values than actual histogram for the fraction of MNPs with a diameter around 100 nm. Although this fraction is small it contributes substantially to the value of the specific surface area.

Figure 3 shows SEM images of commercial CIP particles for the sake of comparison. One can clearly see that CIP particles tend to be spherical but they are approximately an order of magnitude bigger and there is a certain quantity of agglomerates. The average mean diameter of the CIP particles was 1.1 ± 0.4 μm.

Figure 3

3.2. Magnetic characterization

Figure 4 shows the hysteresis loops of both types of the particles. They show a rapid saturation with quite low hysteresis. The EEW MNPs have a saturation magnetization of 190 Am^2/kg, i.e. 7% larger than the CIP microparticles. The value of the saturation magnetization in the bulk state for pure iron is $M_s = 217.6$ Am^2/kg at room temperature [30]. This means that EEW MNPs reach about 87 % of the saturation magnetization of the pure iron in the bulk state. As it was mentioned above, the surface of iron MNPs was passivated prior to exposure to the atmospheric oxygen. In our previous studies [31] we have shown that the passivation oxide layer for low oxygen flow rates is usually about a very few nm. This explains some reduction of the saturation magnetization by the presence of iron oxide shell layer experimentally detected by XRD. Another way to understand the reduction of the saturation magnetization is based on the concept of laws at nanoscale [32]. In the case of pure iron MNPs at least three surface layers are not contributing to the ferromagnetism due to the insufficient number of the nearest neighbours. This can easily explain at least 10 % decay of the saturation magnetization. The main difficulty to make a more precise analysis is caused by the existence of the MNP size distribution and small additions of extra phases (see XRD discussion above).

Figure 4

Coming back to a comparison of magnetic properties of two types of the particles we can suppose that higher saturation magnetization of the EEW is a clear indicator of the higher quality of their compositional and crystalline structure parameters. As is well known [33], intrinsic magnetic properties, as saturation magnetization, are realized on length scales of a few interatomic distances and approach their bulk values on a length scale of about 1 nm. In very small nanoparticles, however, the surface atoms have less neighbors than the inner ones and their magnetic properties are reduced. Experimentally the average magnetization is therefore dependent on the particle size because of the external shell of less interacting atoms and also because of the oxidation of the surface [34,31,32]. This rule, however, doesn't apply in this case because of the different purity of the prepared samples. Commercial samples have less purity and a thicker oxide shell than those prepared by EEW, so the latter display a larger magnetization in spite of their smaller size.

3.2. Magnetorheological characterization

Rheology is the study of flow and deformation of material under applied force, which is measured using a rheometer. In this work we measured rheological properties from bulk sample deformation using a mechanical rheometer. Designed MR fluids showed a non-Newtonian [35] behaviour under application of an external magnetic field. Therefore, the conversion proposed by DIN 53018 [36] between the physical data of the rheometer (rotation speed and torque) and rheological parameters (shear rate and shear stress) was not applicable in the present case. For correct analysis of the data, the Rabinowitsch conversion method has been applied [37]. The magnetic field ranged from 0 to 140 kA/m. After each characterization, a demagnetization cycling procedure was applied.

Both fluids showed a strong magnetorheological response, increasing the shear stress with the magnetic field intensity (Figure 5). The rheological curves of both fluids under an external magnetic field were characterized by the yield stress. The magnitude of the yield stress increases its value with the increase of the magnetic field intensity in both MR fluids. In addition, in both cases, the post-yield behavior can be described as pseudo-plastic.

(Figure 5)

The Herschel-Bulkley model has been used [38] for the parametric description of the rheological post-yield behavior of both magnetic fluids in function of the magnetic field intensity:

$$\tau = \tau_0 + K \times \dot{\gamma}^n \qquad (2),$$

where τ is the shear stress, τ_0 the yield stress, $\dot{\gamma}$ is the shear rate, K the consistency and n the pseudo-plasticity index.

Figure 6 shows the yield stress dependence on the magnetic field intensity of both fluids. The magnetic fluid composed with the EEW MNPs show larger yield stress values comparing with CIP-based fluid in the entire range of the applied magnetic field. This can be explained by the larger value of magnetic saturation of EEW MNPs (Figure 3), as far as the local saturation of the particle magnetization determines the yield stress magnitude [12]. As described by Kim et al. [39], the relationship between the yield stress and the magnetic field intensity is determined by a power law dependency that decreases its value at the critical magnetic field intensity. The fluid composed with the EEW MNPs show a larger critical magnetic field intensity value due to the saturation magnetization.

Figure 6.

Table 1 contains a comparative analysis of the main yield stress values for magnetic fluids reported in literature [11, 40-43] and those in the present work. From the values appearing in the table one can see that, except for those obtained by Noma et. al. [11], the remaining yield stress values are considerably lower than the ones obtained in this work. The results obtained by in Ref. [11], are related to both a larger particle concentration and also larger particle size (104 nm vs 77-80 nm in our case). It can be taken into account that the particles used by Noma et al. have the same value of the saturation magnetization of 190 Am^2/kg, but larger mass and therefore, larger magnetic moment, more than twice our EEW MNPs. Such an increase in magnetic moment can be associated with the increased yield stress. At the same time the larger mass favours the particle sedimentation of the MR fluid. Although large yield stress values are preferred in order to optimize the performance of any MR device, the big particle size affect negatively the fluid stability and a compromise between those two parameters must be achieved.

Table 1.

Coming back to the details of fabrication techniques, the following remarks can be made: EEW particles were obtained with a protective iron oxide coating in the same fabrication chamber using passivation by oxygen. The amount of MNPs, which can be used for preparing the MR fluids without any further treatment, was very high (reaching about one kilogram per batch). The technique is "green", i.e. it does not include water processing. The relatively easy formation of magnetic fluids using EEW MNPs is connected with their very good sphericity, very low amount of defects on the surface and high value of the magnetic moment, considering the size of the particles.

The arc plasma synthesis method for the production of the nanoparticles [11] supposes the particles fabrication in a non-oxidizing environment of Ar–50% and H_2 –50% gas mixture. Such an atmosphere is a reductive one and therefore an oxide layer was formed in the surface. A further treatment in silane was needed to modify the oxide surface and made it appropriate to disperse the nanoparticles into the oil carrier.

5. Conclusions

Iron magnetic nanoparticles have been produced by the high yield technique of the electric explosion of a wire, using pulses providing 130 % the energy of sublimation of metallic iron. XRD analysis confirmed that the major crystalline phase (95 ± 1%) was α-Fe with lattice parameter a = 0.2863(3) nm. The size of coherent diffraction domains of this

phase was 77 ± 3 nm. Two minor phases were found: 2 ± 1% of γ-Fe, cubic bcc (S.G: Fm-3m) with lattice parameter a = 0.3592(2) nm and 3 ± 1% of magnetite (S.G: Fd-3m) with lattice parameter a = 0.8360(6) nm: γ-phase might be associated with small MNPs in the ensemble and magnetite phase corresponds to the passivation layer on the surface of MNPs.

The EEW MNPs presented a larger saturation magnetization value, reaching about 87 % of the saturation magnetization of the iron in the bulk state due to the contributions of the thin passivation layer and the scarce nanoscale size defects. Hence EEW NMPs demonstrated an improved magnetic performance with respect the CIP micron sized particles studied for comparison. The MR fluids composed with the EEW nanoparticles showed larger yield stress (~ 1250 Pa for H = 140 kA/m) values than the MR fluids with CIP micron sized particles (~ 1150 Pa for H = 140 kA/m).

We had proven that the EEW MNPs have a noteworthy potential for MR fluids, showing large yield stress and superior fluid stability. The EEW technique is characterized by reduced energy consumption, a large production rate and the obtained particles being ready for dispersion in the oil carrier for MR fluids applications.

Asknowledgements

J. Berasategi, A. Gomez and M. M. Bou-Ali would like to thank the financial support provided by the Basque Government under ACTIMAT project (KK-2016/00097), PIBA project (PI-2017-1-0055), and Research Group program (IT1009-16). G.V. Kurlyandskaya, J. Gutiérrez and J.M. Barandiarán would like to thank the financial support provided also by the Basque Government under PI-2017-1-0043, the ACTIMAT (ELKARTEK program) and Research Groups IT711-13 research projects. I.V. Beketov, A.P. Safronov and G.V. Kurlyandskaya would like to thank the financial support provided the Ministry of Education and Science of Russia the state task 3.6121.2017/8.9 and Russian Federation state task project 0389-2014-0002. Technical and human support provided by the General Research Services of the UPV/EHU (SGIker) is gratefully acknowledged, as well as URFU Common Services are. We thank A.I. Medvedev and A.M. Murzakaev for special support.

References

[1] Ucar H, Craven M, Laughlin D E, McHenry M E 2014 Effect of Mo additions on structure and magnetocaloric effect in γ -FeNi nanocrystals *J. Elec. Mat.* 43 137–141

[2] de Vicente J, Klingenberg D J, Hidalgo-Alvarez R 2011 Magnetoreological fluids: a review *Soft Matter* ***7*** *3701-10*

[3] Kurlyandskaya G V, Safronov A P, Terzian T V, Volodina N S, Beketov I V, Lezama L, Marcano Prieto L 2015 $Fe_{45}Ni_{55}$ Magnetic Nanoparticles obtained by electric explosion of wire for the development of functional composites *IEEE Magn. Lett.* **6** 3800104

[4] Kotov Yu A 2003 Electric explosion of wires as a method for preparation of nanopowders *J. Nanoparticle Res.* **5** 539–550

[5] Kurlyandskaya G V, Madinabeitia I, Beketov I V, Medvedev A I, Larrañaga A, Safronov A P, Bhagat S M 2014 Structure, magnetic and microwave properties of FeNi nanoparticles obtained by electric explosion of wire *J. Alloys Comp.* **615** S231–S235

[6] Bac L H, Kim B K, Kim J S, Kim J C 2011 Characteristics of Fe-Ni nanopowders prepared by electrical explosion of wire in water and ethanol *J. Mag.*, **16** 435–439

[7] Beketov I V, Safronov A P, Medvedev A I, Alonso J, Kurlyandskaya G V, Bhagat S M 2012 Iron oxide nanoparticles fabricated by electric explosion of wire: Focus on magnetic nanofluids *AIP Adv.* **2** 022154

[8] Agirre-Olabide I, Berasategui J, Elejabarrieta M J, Bou-Ali M M 2014 Characterization of the linear viscoelastic region of magnetorheological elastomers *J. Intel. Mater. Syst. Struct.* **25** 2074-2081

[9] Carlson J D, Jolly M R 2000 MR fluid, foam and elastomer devices *Mechatronics* **10** 555-569

[10] Charles SW; The preparation of magnetic fluids; Stefan Odenbach (Ed.): LNP 594, pp. 3–18, 2002.

[11] Noma J, Abe H, Kikuchi T, Furusho J, Naito M 2010 Magnetorheology of colloidal dispersion containing Fe nanoparticles synthesized bythearc-plasma method *J. Magn. Magn. Mater.* **322** 1868–1871.

[12] Ginder J M, Davis L C 1994 Shear stresses in magnetorheological fluids: Role of magnetic saturation *Appl. Phys. Lett*. **65** 3410-3412.

[13] López-López M T, de Vicente J, Bossis G, González-Caballero F Durán J D G 2005 Preparation of stable magnetorheological fluids based on extremely bimodal iron–magnetite suspensions *J. Mater. Res*. **20** 874-881

[14] Poddar P, Wilson J L, Srikanth H, Yoo J-H, Wereley N M, Kotha S, Barghouty L, Radhakrishnan R 2004 Nanocomposite magneto-rheological fluids with uniformly dispersed Fe nanoparticles *J. Nanosci. Nanotech.* **4** 192–196

[15] Gangopadhyay S, Hadjipanayis G C, Dale B, Sorensen C M, Klabunde K J, Papaefthymiou V, Kostikas A 1992 Magnetic properties of ultrafine iron particles *Phys. Rev. B* **45** 9778–9787

[16] Goncalves F D, Koo J H, Ahmadian M 2006 A review of the state of the art in magnetorheological fluid technologies - Part I: MR fluid and MR fluid models *Shock and Vibration Digest* **38** 203–220

[17] Bell R C, Karli J O, Vavreck A N, Zimmerman D T, Ngatu G T, Wereley N M 2008 Magnetorheology of submicron diameter iron microwires dispersed in silicone oil *Smart Mater. Struct.* **17** 015028.

[18] Kuzhir P, López-López M T, Bossis G 2009 Magnetorheology of fiber suspensions. II. *Theory Journal of Rheology* **53** 127-151.

[19] G. Bossis, O. Volkova, S. Lacis, A. Meunier; Magnetorheology: Fluids, Structures and Rheology in Ferrofluids, edited by S. Odenbach (Springer, Bremen, Germany, 2002), p. 202

[20] de Vicente J, López-López M T, González-Caballero F, Durán J D G 2003 Rheological study of the stabilization of magnetizable colloidal suspensions by addition of silica nanoparticles *J. Rheol.* **47** 1093-1109

[21] Beketov I V, Safronov A P, Bagazeev A V, Larranaga A, Kurlyandskaya G V, Medvedev A I 2014 In situ modification of Fe and Ni magnetic nanopowders produced by the electrical explosion of wire *J. All. Comp.* **586** S483–S488

[22] Shankar A, Safronov A P, Mikhnevich E A, Beketov I V, Kurlyandskaya G V 2017 Ferrogels based on entrapped metallic iron nanoparticles in a polyacrylamide network: extended Derjaguin–Landau–Verwey–Overbeek consideration, interfacial interactions and magnetodeformation *Soft Matter* **13**, 3359

[23] G.V. Kurlyandskaya, S.M. Bhagat, A.P. Safronov, I.V. Beketov, A. Larrañaga, Spherical magnetic nanoparticles fabricated by electric explosion of wire, AIP Advances 1 (2011) 042122.

[24] A.P.Safronov, I.V.Beketov, O.M.Samatov, G.V.Kurlyandskaya, S.M.Bhagat, A.Larranaga, I.Orue, R.Andrade. Nanofluids for biomedical applications using spherical iron oxide magnetic nanoparticles fabricated by high-power physical evaporation. Mater. Matters 2014. V.9 Nº2. P.58-61.

[25] G. V. Kurlyandskaya, A. P. Safronov, T. V. Terzian, N. S. Volodina, I. V. Beketov, L. Lezama, L. Marcano Prieto, Fe45Ni55 Magnetic nanoparticles obtained by electric explosion of wire for the development of functional composites, IEEE Magn. Lett. 6 (2015) 3800104.

[26] P.C. Hiemenz, R. Rajagopalan Principles of Colloid and Surface Chemistry. Marcel Dekker: New York. 1997.

[27] Scherrer P, Bestimmung der Grösse und der inneren Struktur von Kolloidteilchen mittels Röntgensrahlen (Determination of the size and internal structure of colloidal particles using X-rays) 1918 *Nachr. Ges. Wiss. Göttingen* **26** 98–102

[28] http://product-finder.basf.com

[29] P.C. Hiemenz, R. Rajagopalan Principles of Colloid and Surface Chemistry. Marcel Dekker: New York. 1997.

[30] J. Crangle and G.M. Goodman 1971 *Proc. Royal Society of London* **A321** 477-491.

[31] Safronov A P, Kurlyandskaya G V, Chlenova A A, Kuznetsov M V, Bazhin D N, Beketov I V, Sanchez-Ilarduya M B, Martinez-Amesti A, Carbon deposition from aromatic solvents onto active Intact 3d metal surface at ambient conditions 2014 *Langmuir* **30** 3243–3253

[32] Jun Y W, Seo J, Cheon J 2008 Nanoscaling laws of magnetic nanoparticles and their applicabilities in biomedical sciences *Acc. Chem. Res*. **41** 179–189.

[33] Skomski R 2003 Nanomagnetics *J. Phys.: Condens. Matter* 15 R841–R896.

[34] Gangopadhyay S, Hadjipanayis G C, Dale B, Sorensen C M, Klabunde K J, Papaefthymiou V, Kostikas A 1992 Magnetic properties of ultrafine iron particles, *Physical Review B* **45** 9778

[35] Aydar G, Evrensel C A, Gordaninejad F, Fuchs A 2007 A low force magneto-rheological (MR) fluid damper: design, fabrication and characterization *Smart Mater. Struct*. **18** 1155-1160

[36] Deutsches Institut f¨ur Normung 1976 Measurement of the dynamic viscosity of newtonian fluids with rotational viscometers (DIN 53018).

[37] Zubieta M, Elejabarrieta M J, Bou-Ali M M 2009 A numerical method for determining the shear stress of magnetorheological fluids using the parallel-plate measuring system *Rheol. Acta* **48** 89-95.

[38] Mezger TG 2002 The rheology handbook Vincentz Network (Germany).

[39] Kim M H, Choi K, Nam J D, Choi H J 2017 Enhanced magnetorheological response of magnetic chromium dioxide nanoparticle added carbonyl iron suspension *Smart Mater. Struct.* **26** 095006.

[40] Chae H S, Sang Deuk KimS D, Piao S H, Hyoung Jin Choi H J 2016 Core-shell structured Fe_3O_4@SiO_2 nanoparticles fabricated by sol–gel method and their magnetorheology *Colloid Polym. Sci.* **294** 647–655.

[41] Choi H J, Jang I B, Lee J Y, Pich A, Bhattacharya S, Adler H-J 2005 Magnetorheology of synthesized core–shell structured nanoparticle *IEEE Trans. Magn.* **41** 3448-3450.

[42] Kim I G, Song K H, Park B O, Choi B I, Choi H J 2011 Nano-sized Fe soft-magnetic particle and its magnetorheology *Colloid Polym. Sci.* **289** 79–83.

[43] Park B J, Hong M K, Choi H J 2009 Atom transfer radical polymerized PMMA/magnetite nanocomposites and their magnetorheology *Colloid Polym. Sci.* **287** 501–504.

Table 1. Comparison of different MR fluids prepared with micro and nanoparticles.

Reference	**Particle composition**	**Particle size (nm)**	**Particle concentration (wt.%)**	**Carrier**	**Magnetic field (kA/m)**	**Yield stress (Pa)**
This work	Fe (EEW)	85	10	Mineral oil	140	1250
This work	Fe (CIP)	1100	10	Mineral oil	140	1150
[40]	Fe3O4	200	10	silicone oil	137	50
[40]	Fe_3O_4@SiO_2	240	10	silicone oil	137	158
[41]	Fe_3O_4	200	20	silicone oil	171	40
[42]	Fe	4	20	Lubricant oil	343	20
[43]	PMMA/ Fe_3O_4	8-15	10	Yubase8	343	40
[11]	Arc plasma Fe	104	15	Silicone	238	5500
[11]	Fe (arc plasma)	104	15	Silicone	159	3100
[11]	Fe (arc plasma)	104	15	Silicone	79	1500

Figure captions:

Figure 1.

XRD pattern for Fe MNPs (Bruker DISCOVER D8) synthesized via EEW method.

Figure 2.

SEM (a) and TEM (b) images of iron nanoparticles synthesized via EEW method. Inset – particle size distribution obtained by image analysis (histogram) and its lognormal fitting (line).

Figure 3.

SEM image of commercially available micron sized carbonyl iron particles (CIP).

Figure 4.

Hysteresis loops of CIP microparticles and EEW MNPs of iron: EEW MPNs show higher (approximately by 7%) saturation magnetization than CIP microparticles. Inset shows the low field behaviour.

Figure 5.

Rheological curves as a function of the applied magnetic field: 1 – H = 0, 2 – H = 13 kA/m H = 26 kA/m, H = 68 kA/m, H = 140 kA/m. (a) MR fluid with EEW Fe nanoparticles, (b) MR fluid with CIP micron size particles;

Figure 6.

Herschel-Bulkley model parameters for different applied magnetic fields: (a) yield stress, τ_0, (b) consistency *K*, and (c) pseudo-plasticity index, *n*.

Figure 1.

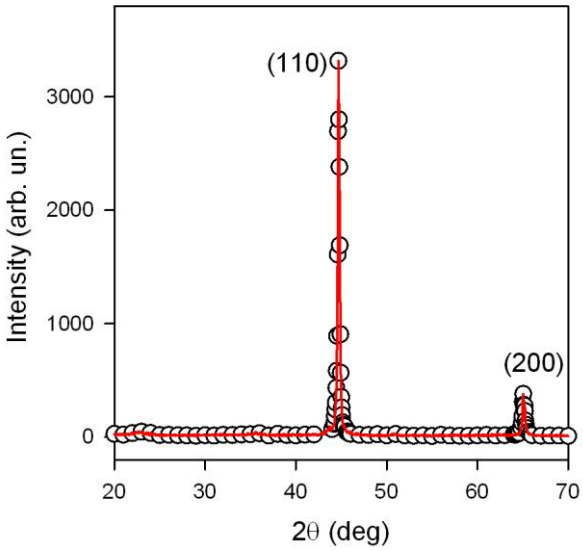
(110)
(200)
Intensity (arb. un.)
3000
2000
1000
0
20
30
40
50
60
70
2θ (deg)

Figure 2.

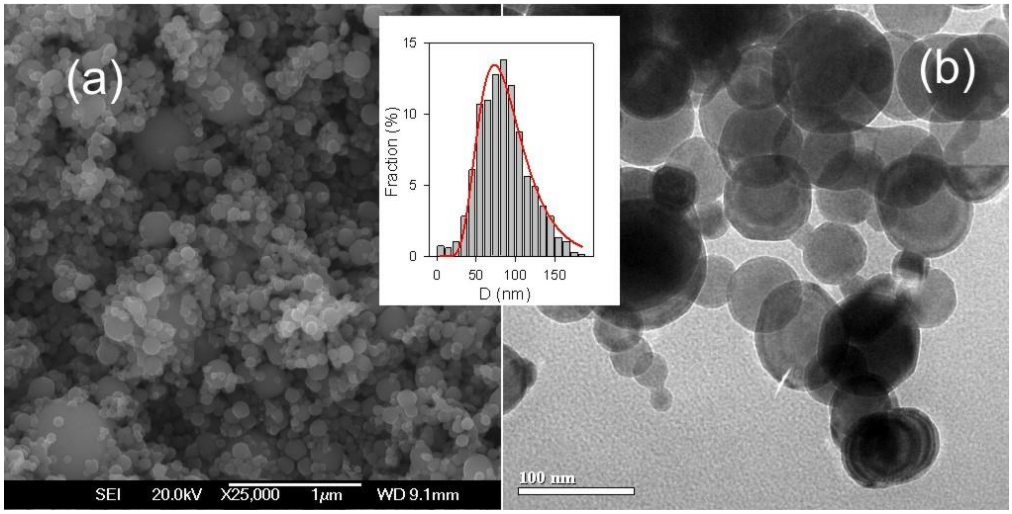
(a)
(b)
Fraction (%)
15
10
5
0
0
50
100
150
D (nm)
SEI 20.0kV X25,000 1μm WD 9.1mm
100 nm

Figure 3.

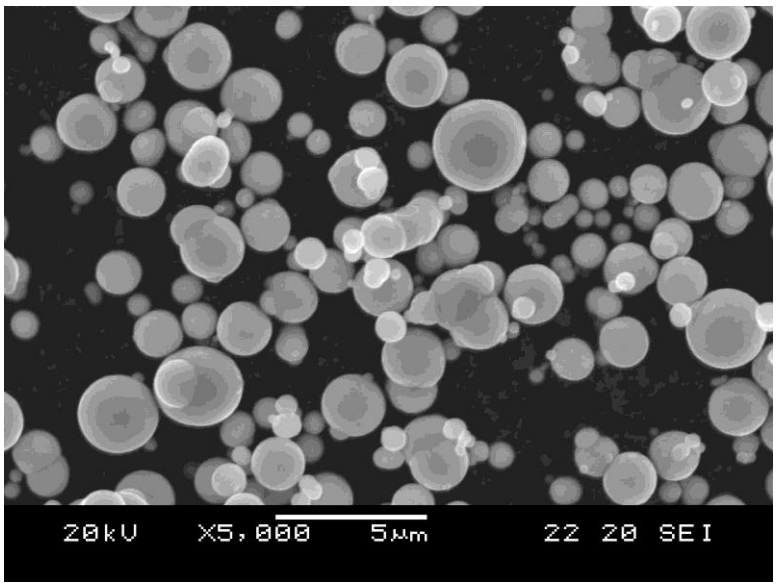

Figure 4.

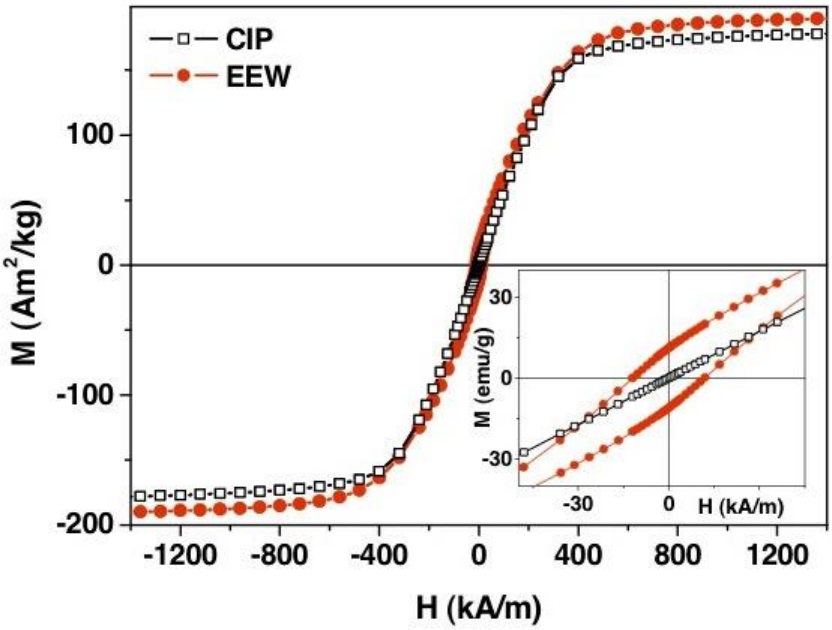
CIP
EEW
M (Am²/kg)
100
0
-100
-200
-1200
-800
-400
0
400
800
1200
H (kA/m)
M (emu/g)
30
0
-30
-30
0
H (kA/m)

Figure 5.

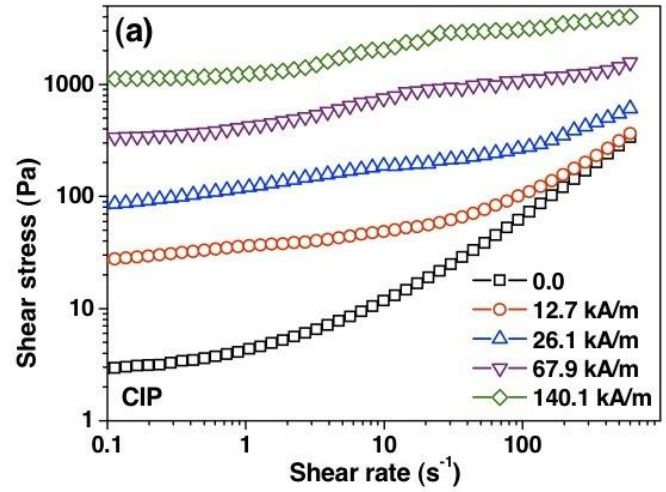
(a)
Shear stress (Pa)
1000
100
10
1
0.1
1
10
100
Shear rate (s-1)
0.0
12.7 kA/m
26.1 kA/m
67.9 kA/m
140.1 kA/m
CIP

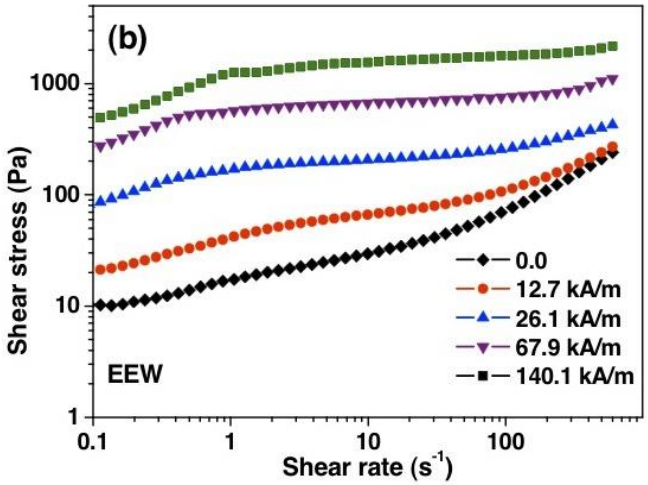
(b)
Shear stress (Pa)
1000
100
10
1
0.1
1
10
100
Shear rate (s-1)
0.0
12.7 kA/m
26.1 kA/m
67.9 kA/m
140.1 kA/m
EEW

Figure 6.

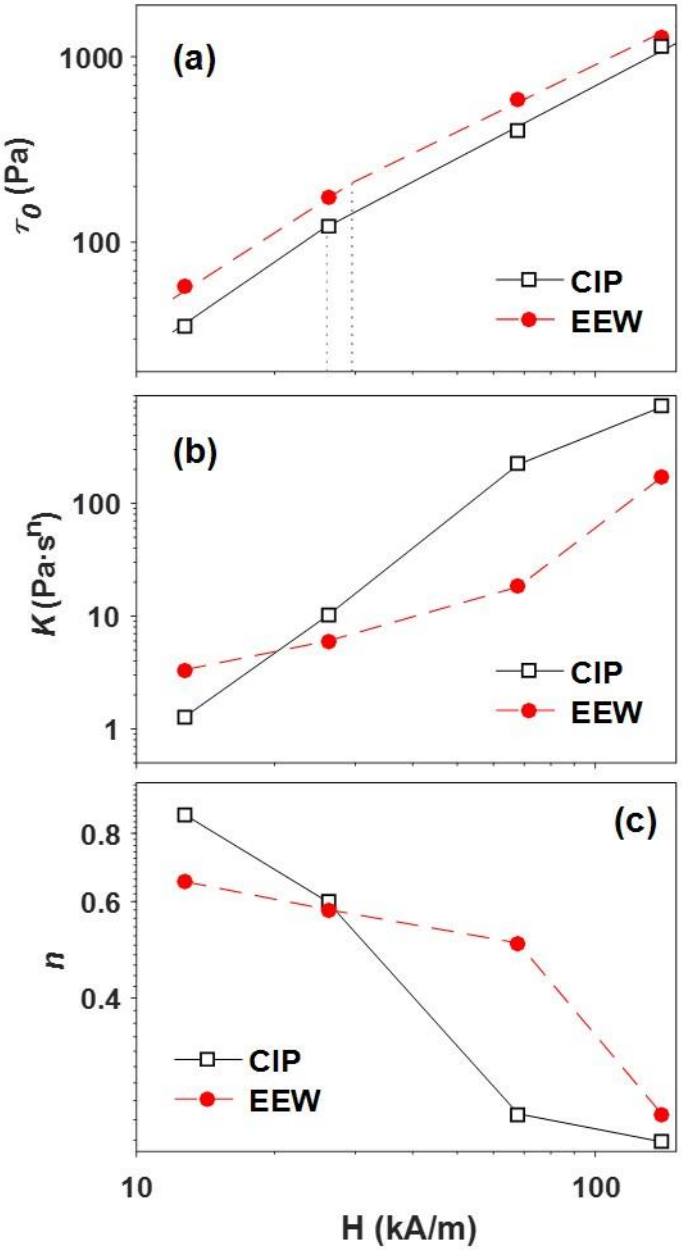
(a)
1000
100
τ_0 (Pa)
CIP
EEW
(b)
100
10
1
K (Pa·s^n)
CIP
EEW
(c)
0.8
0.6
0.4
n
CIP
EEW
10
100
H (kA/m)